Hindawi Publishing Corporation
Journal of Engineering
Volume 2013, Article ID 230120, 18 pages
http://dx.doi.org/10.1155/2013/230120

Research Article

Dynamic Characters of Stiffened Composite Conoidal Shell Roofs with Cutouts: Design Aids and Selection Guidelines

Sarmila Sahoo

Department of Civil Engineering, Heritage Institute of Technology, Kolkata 700107, India

Correspondence should be addressed to Sarmila Sahoo; sarmila_ju@yahoo.com

Received 11 December 2012; Revised 3 May 2013; Accepted 14 May 2013

Academic Editor: Jun Li

Dynamic characteristics of stiffened composite conoidal shells with cutout are analyzed in terms of the natural frequency and mode shapes. A finite element code is developed for the purpose by combining an eight-noded curved shell element with a three-noded curved beam element. The code is validated by solving benchmark problems available in the literature and comparing the results. The size of the cutouts and their positions with respect to the shell centre are varied for different edge constraints of cross-ply and angle-ply laminated composite conoids. The effects of these parametric variations on the fundamental frequencies and mode shapes are considered in details. The results furnished here may be readily used by practicing engineers dealing with stiffened composite conoids with cutouts central or eccentric.

1. Introduction

Laminated composite structures are gaining wide importance in various fields of aerospace and civil engineering. Shell roof structures can be conveniently built with composite materials that have many attributes, besides high specific strength and stiffness. Among the different shell panels which are commonly used as roofing units in civil engineering practice, the conoidal shell has a special position due to a number of advantages it offers. Conoidal shells are often used to cover large column-free areas. Being ruled surfaces, they provide ease of casting and also allow north light in. Hence, this shell is preferred in many places, particularly in medical, chemical, and food processing industries where entry of north light is desirable. Application of conoids in these industries often necessitates cutouts for the passage of light, service lines, and also sometimes for alteration of resonant frequency. In practice, the margin of the cutouts must be stiffened to take account of stress concentration effects. An in-depth study including bending, buckling, vibration, and impact is required to exploit the possibilities of these curved forms. The present investigation is, however, restricted only to the free vibration behaviour. A generalized formulation for the doubly curved laminated composite shell has been presented using the eight-noded curved quadratic isoparametric finite element including three radii of curvature. Some of the important contributions on the investigation of conoidal shells are briefly reviewed here.

The research on conoidal shell started about four decades ago. In 1964, Hadid [1] analysed static characteristics of conoidal shells using the variational method. The research was carried forward and improved by researchers like Brebbia and Hadid [2], Choi [3], Ghosh and Bandyopadhyay [4, 5], Dey et al. [6], and Das and Bandyopadhyay [7]. Dey et al. [6] provided a significant contribution on static analysis of conoidal shell. Chakravorty et al. [8] applied the finite element technique to explore the free vibration characteristics of shallow isotropic conoids and also observed the effects of excluding some of the inertia terms from the mass matrix on the first four natural frequencies. Chakravorty et al. [9–11] published a series of papers where they reported on free and forced vibration characteristics of graphite-epoxy composite conoidal shells with regular boundary conditions. Later, Nayak and Bandyopadhyay [12–15] reported free vibration of stiffened isotropic and composite conoidal shells. Das and Chakravorty [16, 17] considered bending and free vibration characteristics of unpunctured and unstiffened composite conoids. Hota and Chakravorty [18] studied isotropic punctured conoidal shells with complicated boundary conditions along the four edges, but no such study about composite

conoidal shells is available in the literature. Also, they did not furnish any information on vibration mode shapes. It is also seen from the recent reviews [19, 20] that dynamic characteristics of stiffened conoidal shells with cutout are still missing in the literature. The present study thus focuses on the free vibrations of graphite-epoxy laminated composite stiffened conoids with cutout both in terms of the natural frequencies and mode shapes. The results so obtained may be readily used by practicing engineers dealing with stiffened composite conoids with cutouts. The novelty of the present study lies in the consideration of vibration mode shapes of stiffened composite conoids in presence of cutouts.

2. Mathematical Formulation

A laminated composite conoidal shell of uniform thickness h (Figure 1), and radius of curvature R_y, and radius of cross curvature R_{xy} is considered. Keeping the total thickness the same, the thickness may consist of any number of thin laminae each of which may be arbitrarily oriented at an angle θ with reference to the x-axis of the coordinate system. The constitutive equations for the shell are given by (a list of notations is separately given)

$$\{F\} = [E]\{\varepsilon\}, \tag{1}$$

where

$$\{F\} = \left\{N_x, N_y, N_{xy}, M_x, M_y, M_{xy}, Q_x, Q_y\right\}^T,$$
$$[E] = \begin{bmatrix} [A] & [B] & [0] \\ [B] & [D] & [0] \\ [0] & [0] & [S] \end{bmatrix}, \tag{2}$$
$$\{\varepsilon\} = \left\{\varepsilon_x^0, \varepsilon_y^0, \gamma_{xy}^0, k_x, k_{xy}, \gamma_{xz}^0, \gamma_{yz}^0\right\}^T.$$

The force and moment resultants are expressed as

$$\left\{N_x, N_y, N_{xy}, M_x, M_y, M_{xy}, Q_x, Q_y\right\}^T = \int_{-h/2}^{h/2} \left\{\sigma_x, \sigma_y, \tau_{xy}, \sigma_z \cdot z, \sigma_y \cdot z, \tau_{xy} \cdot z, \tau_{xz}, \tau_{yz}\right\}^T dz. \tag{3}$$

The submatrices $[A]$, $[B]$, $[D]$, and $[S]$ of the elasticity matrix $[E]$ are functions of Young's moduli, shear moduli, and Poisson's ratio of the laminates. They also depend on the angle which the individual lamina of a laminate makes with the global x-axis. The detailed expressions of the elements of the elasticity matrix are available in several references including Vasiliev et al. [21] and Qatu [22].

The strain-displacement relations on the basis of improved first-order approximation theory for thin shell (Dey et al. [6]) are established as

$$\left\{\varepsilon_x, \varepsilon_y, \gamma_{xy}, \gamma_{xz}, \gamma_{yz}\right\}^T = \left\{\varepsilon_x^0, \varepsilon_y^0, \gamma_{xy}^0, \gamma_{xz}^0, \gamma_{yz}^0\right\}^T + z\left\{k_x, k_y, k_{xy}, k_{xz}, k_{yz}\right\}^T, \tag{4}$$

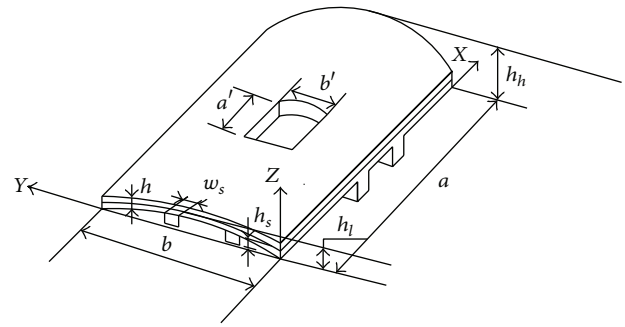

Figure 1: Conoidal shell with a concentric cutout stiffened along the margins.

where the first vector is the midsurface strain for a conoidal shell and the second vector is the curvature.

3. Finite Element Formulation

3.1. Finite Element Formulation for Shell. An eight-noded curved quadratic isoparametric finite element is used for conoidal shell analysis. The five degrees of freedom taken into consideration at each node are u, v, w, α, β. The following expressions establish the relations between the displacement at any point with respect to the coordinates ξ and η and the nodal degrees of freedom

$$u = \sum_{i=1}^{8} N_i u_i, \qquad v = \sum_{i=1}^{8} N_i v_i, \qquad w = \sum_{i=1}^{8} N_i w_i,$$
$$\alpha = \sum_{i=1}^{8} N_i \alpha_i, \qquad \beta = \sum_{i=1}^{8} N_i \beta_i, \tag{5}$$

where the shape functions derived from a cubic interpolation polynomial [6] are

$$N_i = \frac{(1+\xi\xi_i)(1+\eta\eta_i)(\xi\xi_i+\eta\eta_i-1)}{4}, \quad \text{for } i = 1,2,3,4,$$
$$N_i = \frac{(1+\xi\xi_i)(1-\eta^2)}{2}, \quad \text{for } i = 5,7,$$
$$N_i = \frac{(1+\eta\eta_i)(1-\xi^2)}{2}, \quad \text{for } i = 6,8. \tag{6}$$

The generalized displacement vector of an element is expressed in terms of the shape functions and nodal degrees of freedom as

$$[u] = [N]\{d_e\}, \tag{7}$$

that is,

$$\{u\} = \begin{Bmatrix} u \\ v \\ w \\ \alpha \\ \beta \end{Bmatrix} = \sum_{i=1}^{8} \begin{bmatrix} N_i & & & & \\ & N_i & & & \\ & & N_i & & \\ & & & N_i & \\ & & & & N_i \end{bmatrix} \begin{Bmatrix} u_i \\ v_i \\ w_i \\ \alpha_i \\ \beta_i \end{Bmatrix}. \tag{8}$$

3.1.1. Element Stiffness Matrix. The strain-displacement relation is given by

$$\{\varepsilon\} = [B]\{d_e\}, \tag{9}$$

where

$$[B] = \sum_{i=1}^{8} \begin{bmatrix} N_{i,x} & 0 & 0 & 0 & 0 \\ 0 & N_{i,y} & -\dfrac{N_i}{R_y} & 0 & 0 \\ N_{i,y} & N_{i,x} & -\dfrac{2N_i}{R_{xy}} & 0 & 0 \\ 0 & 0 & 0 & N_{i,x} & 0 \\ 0 & 0 & 0 & 0 & N_{i,y} \\ 0 & 0 & 0 & N_{i,y} & N_{i,x} \\ 0 & 0 & N_{i,x} & N_i & 0 \\ 0 & 0 & N_{i,y} & 0 & N_i \end{bmatrix}. \tag{10}$$

The element stiffness matrix is

$$[K_e] = \iint [B]^T [E][B]\, dx\, dy. \tag{11}$$

3.1.2. Element Mass Matrix. The element mass matrix is obtained from the integral

$$[M_e] = \iint [N]^T [P][N]\, dx\, dy, \tag{12}$$

where

$$[N] = \sum_{i=1}^{8} \begin{bmatrix} N_i & 0 & 0 & 0 & 0 \\ 0 & N_i & 0 & 0 & 0 \\ 0 & 0 & N_i & 0 & 0 \\ 0 & 0 & 0 & N_i & 0 \\ 0 & 0 & 0 & 0 & N_i \end{bmatrix},$$
$$[P] = \sum_{i=1}^{8} \begin{bmatrix} P & 0 & 0 & 0 & 0 \\ 0 & P & 0 & 0 & 0 \\ 0 & 0 & P & 0 & 0 \\ 0 & 0 & 0 & I & 0 \\ 0 & 0 & 0 & 0 & I \end{bmatrix}, \tag{13}$$

in which

$$P = \sum_{k=1}^{np} \int_{z_{k-1}}^{z_k} \rho\, dz, \qquad I = \sum_{k=1}^{np} \int_{z_{k-1}}^{z_k} z\rho\, dz. \tag{14}$$

3.2. Finite Element Formulation for Stiffener of the Shell. Three-noded curved isoparametric beam element (Figure 2) are used to model the stiffeners, which are taken to run only along the boundaries of the shell elements. In the stiffener element, each node has four degrees of freedom, that is, u_{sx}, w_{sx}, α_{sx}, and β_{sx} for X-stiffener and v_{sy}, w_{sy}, α_{sy}, and β_{sy} for Y-stiffener. The generalized force-displacement relation of stiffeners can be expressed as

$$X\text{-stiffener: } \{F_{sx}\} = [D_{sx}]\{\varepsilon_{sx}\} = [D_{sx}][B_{sx}]\{\delta_{sxi}\},$$
$$Y\text{-stiffener: } \{F_{sy}\} = [D_{sy}]\{\varepsilon_{sy}\} = [D_{sy}][B_{sy}]\{\delta_{syi}\}, \tag{15}$$

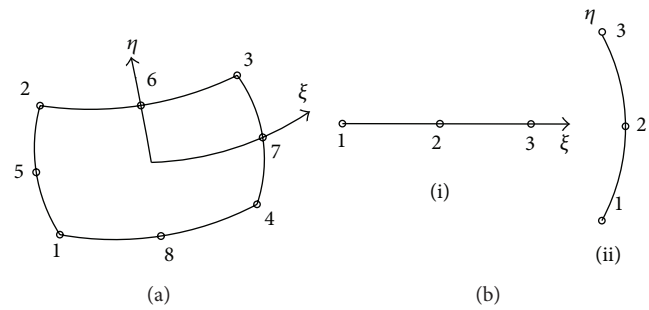

Figure 2: (a) Eight-noded shell element with isoparametric coordinates. (b) Three-noded stiffener element: (i) X-stiffener (ii) Y-stiffener.

where

$$\{F_{sx}\} = [N_{sxx}\ \ M_{sxx}\ \ T_{sxx}\ \ Q_{sxxz}]^T,$$
$$\{\varepsilon_{sx}\} = [u_{sx\cdot x}\ \ \alpha_{sx\cdot x}\ \ \beta_{sx\cdot x}\ \ (\alpha_{sx} + w_{sx\cdot x})]^T,$$
$$\{F_{sy}\} = [N_{syy}\ \ M_{syy}\ \ T_{syy}\ \ Q_{syyz}]^T,$$
$$\{\varepsilon_{sy}\} = [v_{sy\cdot y}\ \ \beta_{sy\cdot y}\ \ \alpha_{sy\cdot y}\ \ (\beta_{sy} + w_{sy\cdot y})]^T. \tag{16}$$

The generalized displacements of the Y-stiffener and the shell are related by the transformation matrix $\{\delta_{syi}\} = [T]\{\delta\}$, where

$$[T] = \begin{bmatrix} 1 + \dfrac{e}{R_y} & \text{symmetric} & & \\ 0 & 1 & & \\ 0 & 0 & 1 & \\ 0 & 0 & 0 & 1 \end{bmatrix}. \tag{17}$$

This transformation is required due to curvature of Y-stiffener, and $\{\delta\}$ is the appropriate portion of the displacement vector of the shell excluding the displacement component along the x-axis.

Elasticity matrices are as follows:

$$[D_{sx}] = \begin{bmatrix} A_{11}b_{sx} & B'_{11}b_{sx} & B'_{12}b_{sx} & 0 \\ B'_{11}b_{sx} & D'_{11}b_{sx} & D'_{12}b_{sx} & 0 \\ B'_{12}b_{sx} & D'_{12}b_{sx} & \dfrac{1}{6}(Q_{44} + Q_{66})\, d_{sx}b_{sx}^3 & 0 \\ 0 & 0 & 0 & b_{sx}S_{11} \end{bmatrix},$$
$$[D_{sy}] = \begin{bmatrix} A_{22}b_{sy} & B'_{22}b_{sy} & B'_{12}b_{sy} & 0 \\ B'_{22}b_{sy} & \dfrac{1}{6}(Q_{44} + Q_{66})\, b_{sy} & D'_{12}b_{sy} & 0 \\ B'_{12}b_{sy} & D'_{12}b_{sy} & D'_{11}d_{sy}b_{sy}^3 & 0 \\ 0 & 0 & 0 & b_{sy}S_{22} \end{bmatrix}, \tag{18}$$

where

$$D'_{ij} = D_{ij} + 2eB_{ij} + e^2 A_{ij},$$
$$B'_{ij} = B_{ij} + eA_{ij}, \tag{19}$$

and A_{ij}, B_{ij}, D_{ij}, and S_{ij} are explained in an earlier paper by Sahoo and Chakravorty [23].

Here, the shear correction factor is taken as 5/6. The sectional parameters are calculated with respect to the mid-surface of the shell by which the effect of eccentricities of stiffeners is automatically included. The element stiffness matrices are of the following forms:

$$\begin{aligned} &\text{for } X\text{-stiffener: } [K_{xe}] = \int [B_{sx}]^T [D_{sx}] [B_{sx}]\, dx, \\ &\text{for } Y\text{-stiffener: } [K_{ye}] = \int [B_{sy}]^T [D_{sy}] [B_{sy}]\, dy. \end{aligned} \tag{20}$$

The integrals are converted to isoparametric coordinates and are carried out by 2-point Gauss quadrature. Finally, the element stiffness matrix of the stiffened shell is obtained by appropriate matching of the nodes of the stiffener and shell elements through the connectivity matrix and is given as

$$[K_e] = [K_{\text{she}}] + [K_{xe}] + [K_{ye}]. \tag{21}$$

The element stiffness matrices are assembled to get the global matrices.

3.2.1. Element Mass Matrix. The element mass matrix for shell is obtained from the integral

$$[M_e] = \iint [N]^T [P] [N]\, dx\, dy, \tag{22}$$

where

$$\begin{aligned} [N] &= \sum_{i=1}^{8} \begin{bmatrix} N_i & 0 & 0 & 0 & 0 \\ 0 & N_i & 0 & 0 & 0 \\ 0 & 0 & N_i & 0 & 0 \\ 0 & 0 & 0 & N_i & 0 \\ 0 & 0 & 0 & 0 & N_i \end{bmatrix}, \\ [P] &= \sum_{i=1}^{8} \begin{bmatrix} P & 0 & 0 & 0 & 0 \\ 0 & P & 0 & 0 & 0 \\ 0 & 0 & P & 0 & 0 \\ 0 & 0 & 0 & I & 0 \\ 0 & 0 & 0 & 0 & I \end{bmatrix}, \end{aligned} \tag{23}$$

in which

$$P = \sum_{k=1}^{np} \int_{z_{k-1}}^{z_k} \rho\, dz, \qquad I = \sum_{k=1}^{np} \int_{z_{k-1}}^{z_k} z\rho\, dz. \tag{24}$$

Element mass matrix for stiffener element

$$\begin{aligned} [M_{sx}] &= \iint [N]^T [P] [N]\, dx \quad \text{for } X\text{-stiffener}, \\ [M_{sy}] &= \iint [N]^T [P] [N]\, dy \quad \text{for } Y\text{-stiffener}. \end{aligned} \tag{25}$$

Here, $[N]$ is a 3×3 diagonal matrix.

Consider

$$[P] = \sum_{i=1}^{3} \begin{bmatrix} \rho \cdot b_{sx} d_{sx} & 0 & 0 & 0 \\ 0 & \rho \cdot b_{sx} d_{sx} & 0 & 0 \\ 0 & 0 & \dfrac{\rho \cdot b_{sx} d_{sx}^2}{12} & 0 \\ 0 & 0 & 0 & \dfrac{\rho\left(b_{sx} \cdot d_{sx}^3 + b_{sx}^3 \cdot d_{sx}\right)}{12} \end{bmatrix}$$

for X-stiffener,

$$[P] = \sum_{i=1}^{3} \begin{bmatrix} \rho \cdot b_{sy} d_{sy} & 0 & 0 & 0 \\ 0 & \rho \cdot b_{sy} d_{sy} & 0 & 0 \\ 0 & 0 & \dfrac{\rho \cdot b_{sy} d_{sy}^2}{12} & 0 \\ 0 & 0 & 0 & \dfrac{\rho\left(b_{sy} \cdot d_{sy}^3 + b_{sy}^3 \cdot d_{sy}\right)}{12} \end{bmatrix}$$

for Y-stiffener. (26)

The mass matrix of the stiffened shell element is the sum of the matrices of the shell and the stiffeners matched at the appropriate nodes

$$[M_e] = [M_{\text{she}}] + [M_{xe}] + [M_{ye}]. \tag{27}$$

The element mass matrices are assembled to get the global matrices.

3.3. Modeling the Cutout. The code developed can take the position and size of cutout as input. The program is capable of generating nonuniform finite element mesh all over the shell surface. So, the element size is gradually decreased near the cutout margins. One such typical mesh arrangement is shown in Figure 3. Such finite element mesh is redefined in steps, and a particular grid is chosen to obtain the fundamental frequency when the result does not improve by more than one percent on further refining. Convergence of results is ensured in all the problems taken up here.

3.4. Solution Procedure for Free Vibration Analysis. The free vibration analysis involves determination of natural frequencies from the condition

$$\left|[K] - \omega^2 [M]\right| = 0. \tag{28}$$

This is a generalized eigen value problem and is solved by the subspace iteration algorithm.

4. Numerical Examples

The validity of the present approach is checked through solution of benchmark problems. The first problem, free vibration of stiffened clamped conoid, was solved earlier by Nayak and Bandyopadhyay [13]. The second is the free vibration of composite conoid with cutouts solved by Chakravorty et al. [11]. The results obtained by the present method, along with the published results, are presented in Tables 1 and 2, respectively.

Additional problems for conoids with cutouts are solved, varying the size and position of cutout along both of the plan

Table 1: Fundamental frequencies (rad/sec) of clamped conoidal shell with central stiffeners.

Stiffener position	Stiffener along x-direction				Stiffener along y-direction				Stiffener along both x- and y-directions			
	Nayak and Bandyopadhyay [13]	Present model			Nayak and Bandyopadhyay [13]	Present model			Nayak and Bandyopadhyay [13]	Present model		
		8×8	10×10	12×12		8×8	10×10	12×12		8×8	10×10	12×12
Concentric	17.28	17.50	17.37	17.31	20.83	21.15	20.85	20.76	20.90	21.24	21.01	20.84
Eccentric at top	17.83	17.92	17.78	17.73	21.57	21.76	21.53	21.45	22.39	22.86	22.51	22.32
Eccentric at bottom	17.55	17.80	17.61	17.52	22.31	22.66	22.40	22.24	22.92	23.25	23.00	22.87

$a = 50$ m, $b = 50$ m, $h = 0.2$ m, $h_h = 10$ m, $h_l = 2.5$ m, $E = 25.4910 \times 10^9$, $\nu = 0.15$, $\rho = 2500$ kg/m^3, $w_s = 0.3$ m, and $h_s = 1$ m.

Table 2: Nondimensional fundamental frequencies ($\overline{\omega}$) for laminated composite conoidal shell with cutout.

a'/a	Corner point supported		Simply supported		Clamped	
	Chakravorty et al. [11]	Present model	Chakravorty et al. [11]	Present model	Chakravorty et al. [11]	Present model
0.0	23.863	23.494	75.450	74.892	124.736	123.306
0.1	23.554	23.872	75.098	75.278	123.811	123.987
0.2	23.746	23.485	73.668	73.324	122.074	120.588
0.3	23.510	23.768	69.979	69.763	120.515	119.101
0.4	23.205	23.101	61.824	61.524	116.924	115.924

$a/b = 1$, $a/h = 100$, $a'/b' = 1$, $a/h_h = 2.5$, and $h_l/h_h = 0.25$.

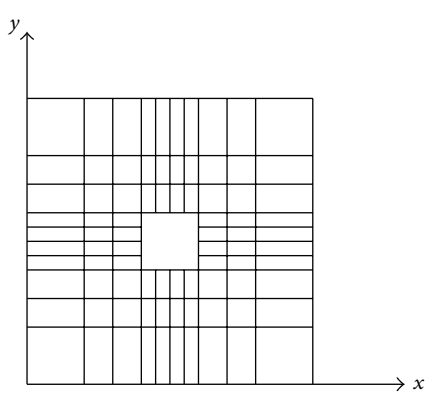

Figure 3: Typical 10×10 nonuniform mesh arrangements drawn to scale.

directions of the shell for different practical boundary conditions. In order to study the effect of cutout size on the free vibration response, results for unpunctured conoids are also included in the study.

5. Results and Discussion

It is found from Table 1 that the fundamental frequencies of stiffened conoids obtained by the present method agree well with those reported by Nayak and Bandyopadhyay [13]. Here, monotonic convergence is noted as the mesh is made progressively finer. Thus, the correctness of the stiffened shell element used here is established. It is evident from Table 2 that the present results agree with those of Chakravorty et al. [11], and the fact that the cutouts are properly modeled in the present formulation is thus established.

5.1. Free Vibration Behaviour of Shells with Concentric Cutouts. Tables 3 and 4 show the results for the non-dimensional fundamental frequency $\overline{\omega}$ of composite cross-ply and angle-ply stiffened conoidal shells for different cutout sizes and various combinations of boundary conditions along the four edges. The shells considered are of square planform ($a = b$), and the cutouts are also taken to be square in plan ($a' = b'$). The cutout sizes (i.e., a'/a) are varied from 0 to 0.4, and boundary conditions are varied along the four edges. Cutouts are concentric on shell surface. The stiffeners are placed along the cutout periphery and extended up to the edge of the shell. The boundary conditions are designated by describing the support clamped or simply supported as C or S taken in an anticlockwise order from the edge $x = 0$. This means that a shell with CSCS boundary is clamped along $x = 0$, simply supported along $y = 0$, clamped along $x = a$, and simply supported along $y = b$. The material and geometric properties of shells and cutouts are mentioned along with the figures.

5.1.1. Effect of Cutout Size on Fundamental Frequency. From Tables 3 and 4, it is seen that when a cutout is introduced to a stiffened shell, the fundamental frequencies increase. This increasing trend continues up to $a'/a = 0.4$ for both cross- and angle ply shells except some angle ply shells with $a'/a > 0.2$. The initial increase in frequency may be explained by the fact that when a cutout is introduced to an unpunctured surface, the number of stiffeners increases from two to four in the present study. When the cutout size is further increased, the number and dimensions of the stiffeners do not change, but the shell surface undergoes loss of both mass and stiffness. As the cutout grows in size, the loss of mass is more significant than that of stiffness, and hence

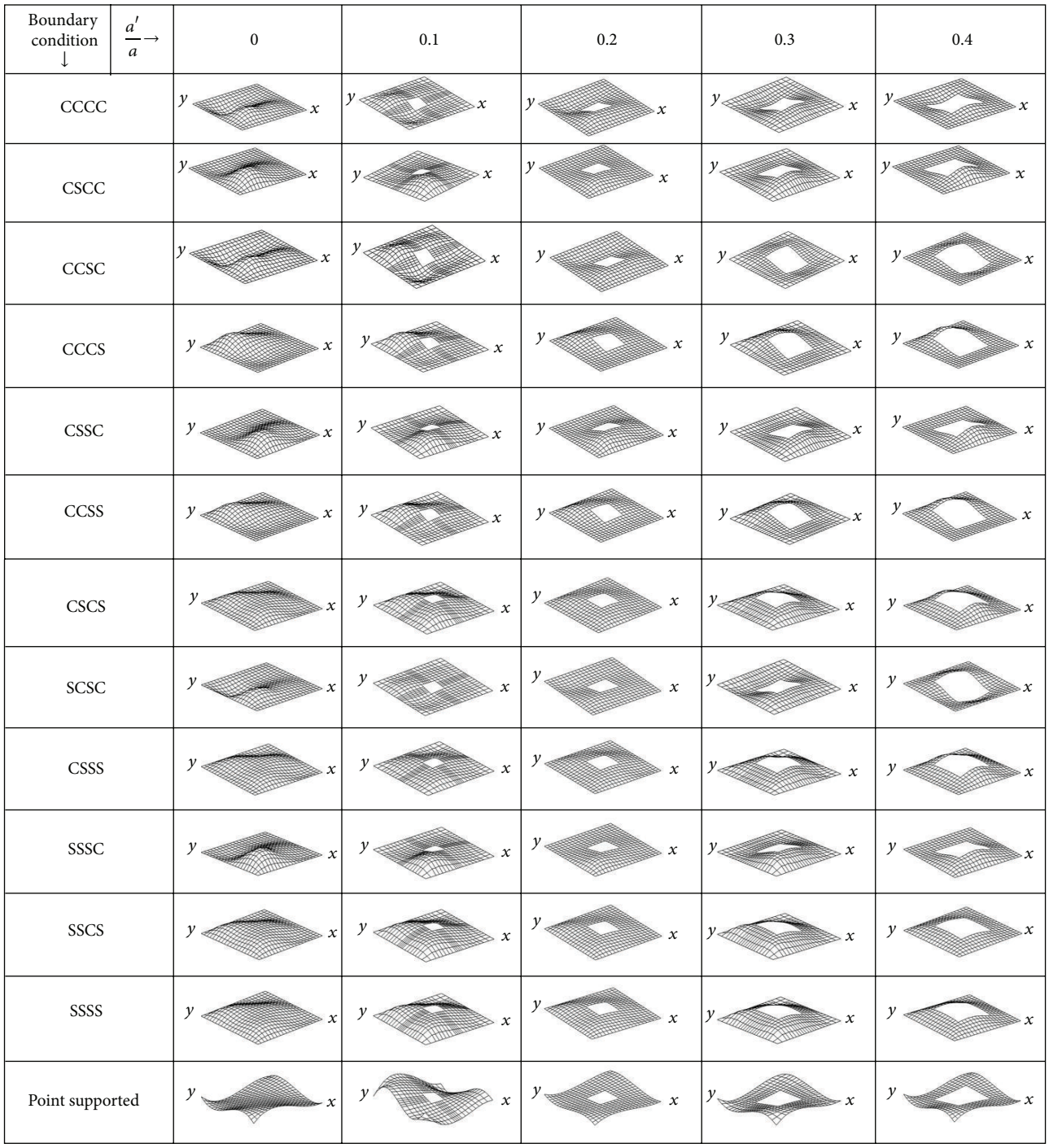

Figure 4: First mode shapes of laminated composite (0/90/0/90) stiffened conoidal shell for different sizes of the central square cutout and boundary conditions.

the frequency increases. But for some angle ply shells with further increase in the size of the cutout, the loss of stiffness gradually becomes more important than that of mass, resulting in decrease in fundamental frequency. This leads to the engineering conclusion that cutouts with stiffened margins may always safely be provided on shell surfaces for functional requirements.

5.1.2. Effect of Boundary Conditions on Fundamental Frequency. The boundary conditions may be divided into six groups, considering number of boundary constraints. The combinations in a particular group have equal number of boundary reactions. These groups are

Group I: CCCC shells,

Group II: CSCC, CCSC, and SCCC shells,

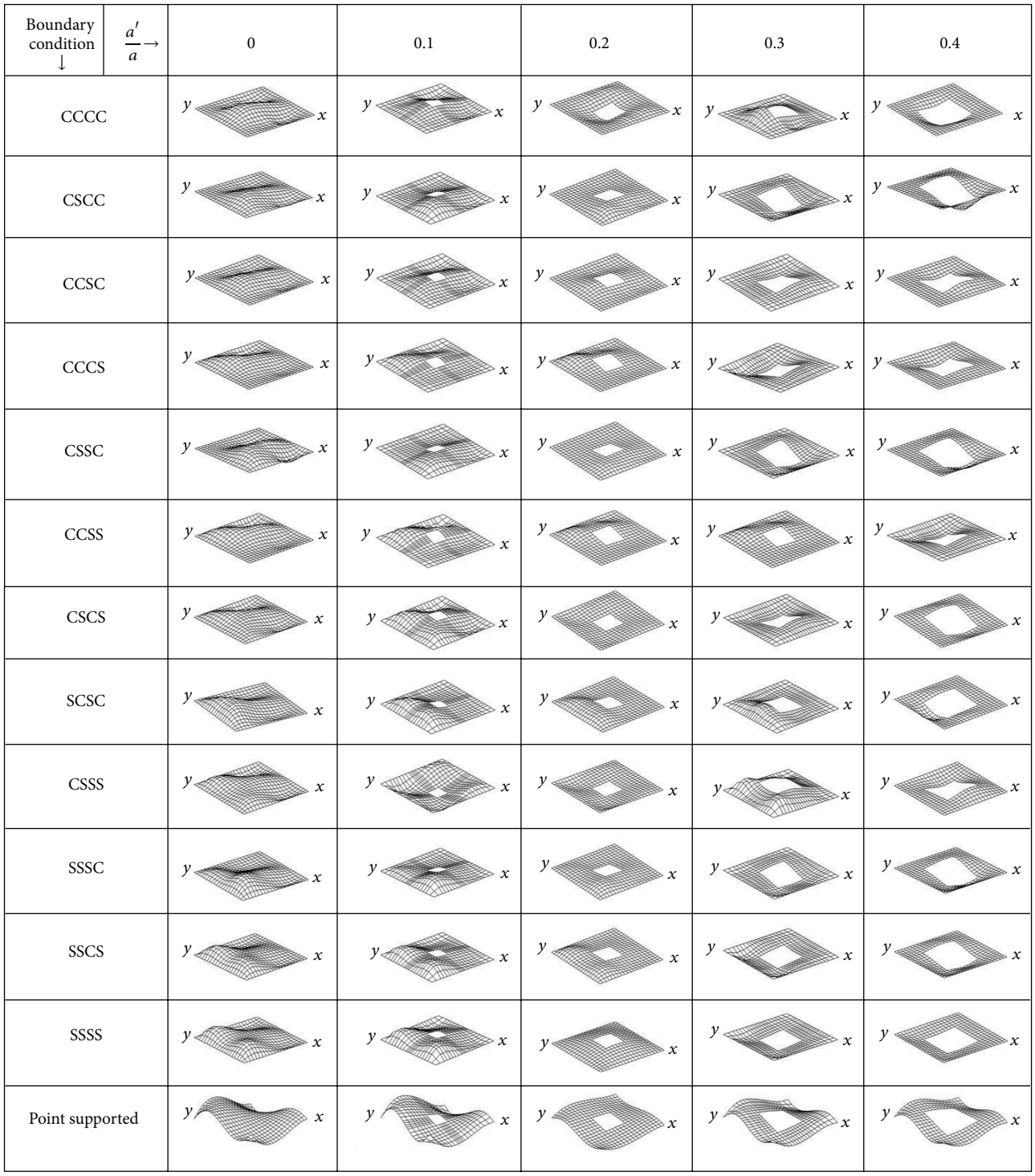

Figure 5: First mode shapes of laminated composite (+45/−45/+45/−45) stiffened conoidal shell for different sizes of the central square cutout and boundary conditions.

Group III: CSSC, SSCC, CSCS, and SCSC shells,

Group IV: CSSS, SSSC, and SSCS shells,

Group V: SSSS shells,

Group VI: Corner point supported shell.

It is seen from Tables 3 and 4 that fundamental frequencies of members belonging to the same groups of boundary combinations may not have close values. So, the different boundary conditions may be regrouped according to performance. According to the values of $\overline{\omega}$, the following groups may be identified.

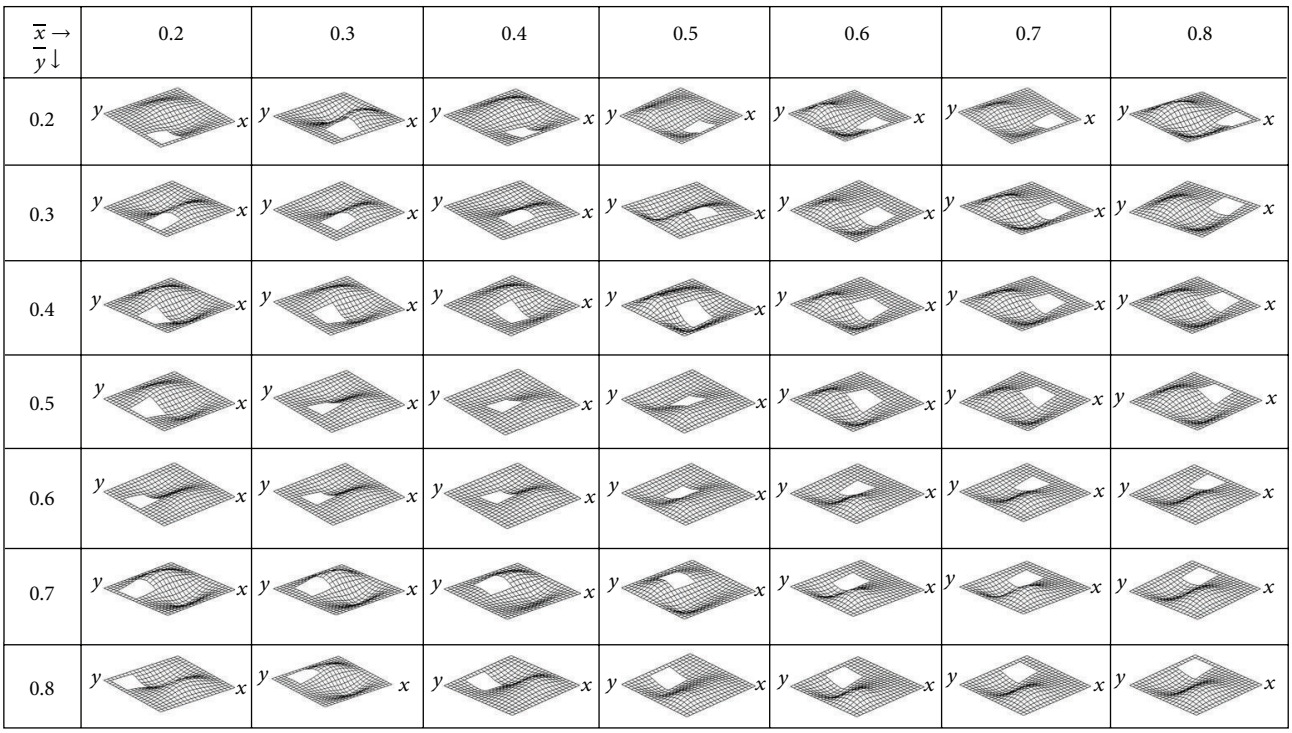

Figure 6: First mode shapes of laminated composite (0/90/0/90) stiffened conoidal shell for different positions of the square cutout with CCCC boundary condition.

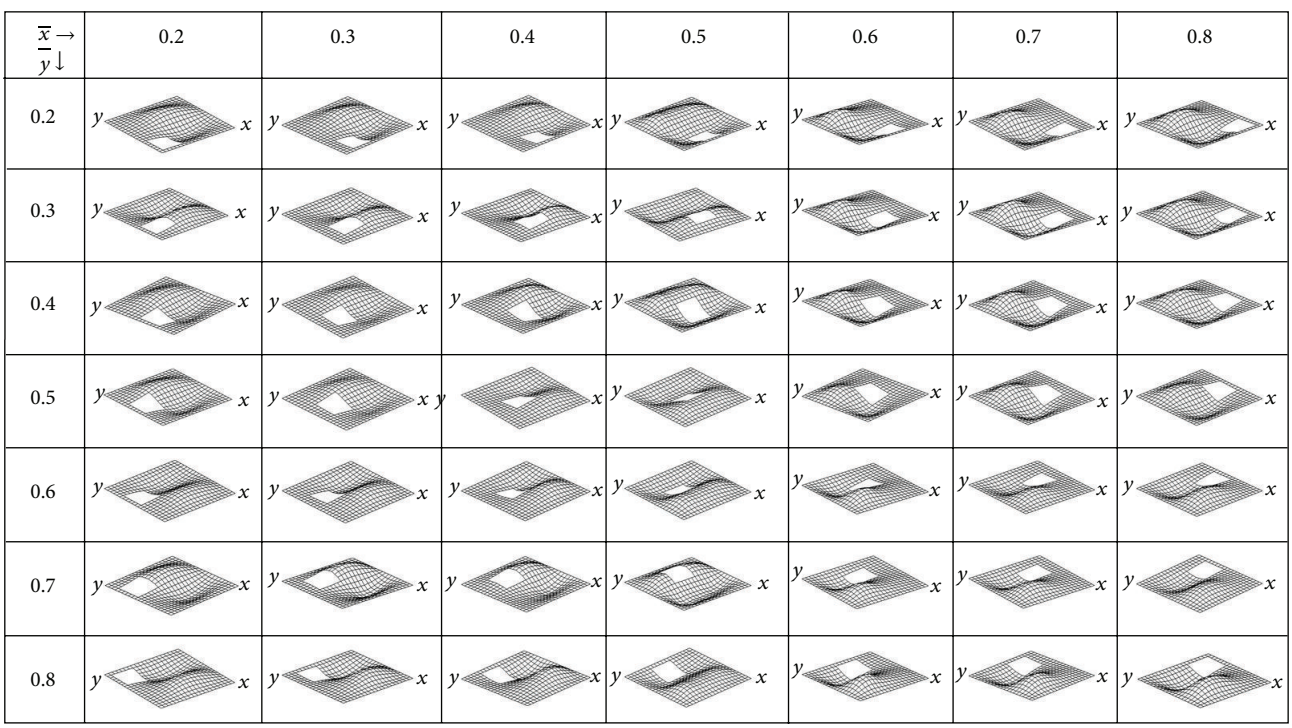

Figure 7: First mode shapes of laminated composite (0/90/0/90) stiffened conoidal shell for different positions of the square cutout with CCSC boundary condition.

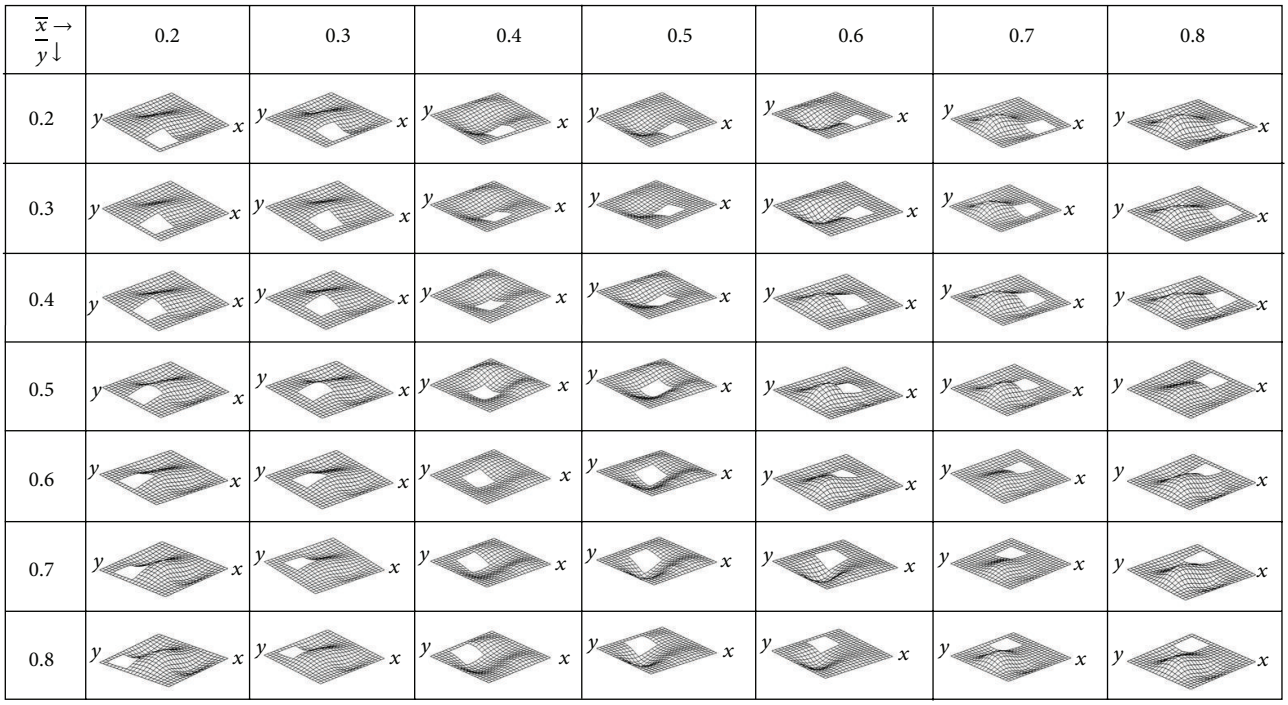

Figure 8: First mode shapes of laminated composite (+45/−45/+45/−45) stiffened conoidal shell for different positions of the square cutout with CCCC boundary condition.

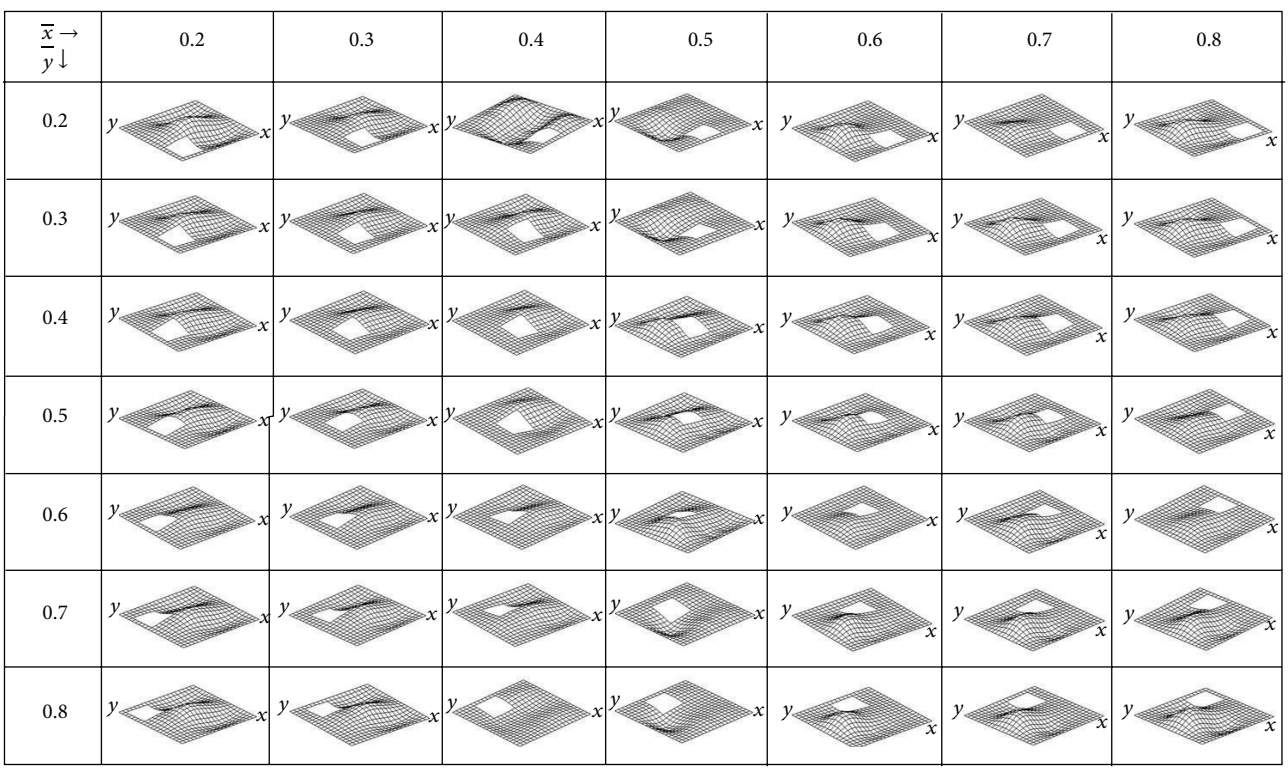

Figure 9: First mode shapes of laminated composite (+45/−45/+45/−45) stiffened conoidal shell for different positions of the square cutout with CCSC boundary condition.

Table 3: Non-dimensional fundamental frequencies ($\overline{\omega}$) for laminated composite (0/90/0/90) stiffened conoidal shell for different sizes of the central square cutout and different boundary conditions.

Boundary conditions	Cutout size (a'/a)				
	0	0.1	0.2	0.3	0.4
CCCC	105.7679	118.9136	124.386	127.4786	124.4929
CSCC	79.3544	87.8992	91.4718	96.4778	97.0499
CCSC	104.0259	117.3182	120.8486	122.5918	119.586
CCCS	79.0009	86.457	91.1477	95.8592	97.0069
CSSC	76.7919	84.417	87.445	91.1546	90.359
CCSS	76.4645	83.126	87.1684	90.6361	90.3194
CSCS	70.8733	76.0322	80.215	86.5974	91.9972
SCSC	96.4607	106.1886	112.2644	116.5409	114.8718
CSSS	65.7562	69.5302	72.8659	77.5964	81.1403
SSSC	65.7398	70.72	75.0802	79.9808	82.2204
SSCS	62.3308	65.2487	69.3811	74.7187	80.4246
SSSS	54.7734	56.6793	59.276	62.3683	65.2097
Point supported	21.1813	21.686	22.6166	24.2309	25.5361

$a/b = 1$, $a/h = 100$, $a'/b' = 1$, $a/h_h = 5$, $h_l/h_h = 0.25$, $E_{11}/E_{22} = 25$, $G_{23} = 0.2E_{22}$, $G_{13} = G_{12} = 0.5E_{22}$, and $\nu_{12} = \nu_{21} = 0.25$.

Table 4: Non-dimensional fundamental frequencies ($\overline{\omega}$) for laminated composite (+45/−45/+45/−45) stiffened conoidal shell for different sizes of the central square cutout and different boundary conditions.

Boundary conditions	Cutout size (a'/a)				
	0	0.1	0.2	0.3	0.4
CCCC	137.5363	149.748	156.932	154.6134	147.0345
CSCC	127.6366	139.9845	142.6213	142.2069	133.7437
CCSC	133.1847	157.494	165.9908	157.6214	149.8912
CCCS	123.9139	136.05	139.2721	140.9553	134.9193
CSSC	119.3132	129.2799	129.5345	119.8123	107.4374
CCSS	114.1784	124.2418	126.9562	119.4147	107.3405
CSCS	119.1939	129.2601	133.1178	136.9644	128.4247
SCSC	117.6296	129.2476	135.318	141.1146	143.7385
CSSS	102.7485	106.9623	109.5824	110.3696	103.1902
SSSC	105.2055	111.0251	113.482	110.7912	101.8345
SSCS	103.0713	107.6771	111.8604	118.8297	123.5415
SSSS	89.8159	91.6626	94.3912	89.284	83.3021
Point supported	26.4022	26.8267	27.3666	28.542	30.1836

$a/b = 1$, $a/h = 100$, $a'/b' = 1$, $a/h_h = 5$, $h_l/h_h = 0.25$, $E_{11}/E_{22} = 25$, $G_{23} = 0.2E_{22}$, $G_{13} = G_{12} = 0.5E_{22}$, and $\nu_{12} = \nu_{21} = 0.25$.

For cross ply shells

Group 1: Contains CCCC, CCSC, and SCSC boundaries which exhibit relatively high frequencies.

Group 2: Contains CSCC, CCCS, CSSC, CCSS, CSCS, SSSC, CSSS, and SSCS which exhibit intermediate values of frequencies.

Group 3: Contains SSSS and corner point supported boundaries which exhibit relatively low values of frequencies.

Similarly for angle ply shells:

Group 1: Contains CCCC, CCSC, CSCC, CCCS, CSSC, CCSS, SCSC, and CSCS boundaries which exhibit relatively high frequencies.

Group 2: Contains SSSC, CSSS, SSCS, and SSSS boundaries which exhibit intermediate values of frequencies.

Group 3: Contains corner point supported shells which exhibit relatively low values of frequencies.

It is evident from the present study that the free vibration characteristics mostly depend on the arrangement of boundary constraints rather than their actual number. It can be seen from the present study that if the higher parabolic edge along $x = a$ is released from clamped to simply supported, there is hardly any change of frequency for cross ply shell. But for angle ply shells, if the edge along higher parabolic edge is released, fundamental frequency even increases more than that of a clamped shell. For cross ply shells, if the edge along $y = 0$ or $y = b$ is released, that is, along the straight edges, frequency values undergo marked decrease. The results indicate that the edge along $y = 0$ or $y = b$ should preferably be clamped in order to achieve higher frequency values, and if the edge has to be released for functional reason, the edge along $x = 0$ and $x = a$ of a conoid must be clamped to make up for the loss of frequency. But for angle ply shells, if any two edges are released, the change in fundamental frequency is not so significant.

Tables 5 and 6 show the efficiency of a particular clamping option in improving the fundamental frequency of a shell with minimum number of boundary constraints relative to that of a clamped shell. Marks are assigned to each boundary combination in a scale assigning a value of 0 to the frequency of a corner point supported shell and 100 to that of a fully clamped shell. These marks are furnished for cutouts with $a'/a = 0.2$ These tables will enable a practicing engineer to realize at a glance the efficiency of a particular boundary condition in improving the frequency of a shell, taking that of clamped shell as the upper limit.

5.1.3. Mode Shapes. The mode shapes corresponding to the fundamental modes of vibration are plotted in Figures 4 and 5 for cross-ply and angle ply shells, respectively. The normalized displacements are drawn with the shell midsurface as the reference for all the support conditions and for all the laminations used here. The fundamental mode is clearly a bending mode for all the boundary conditions for cross-ply and angle-ply shells, except for corner point supported shell. For corner point supported shells, the fundamental mode shapes are complicated. With the introduction of cutout, mode shapes remain almost similar. When the size of the cutout is increased from 0.2 to 0.4, the fundamental modes of vibration do not change to an appreciable amount.

Table 5: Clamping options for 0/90/0/90 conoidal shells with central cutouts having a'/a ratio 0.2.

Number of sides to be clamped	Clamped edges	Improvement of frequencies with respect to point supported shells	Marks indicating the efficiencies of number of restraints
0	Corner point supported	—	0
0	Simply supported no edges clamped (SSSS)	Good improvement	35
1	(a) Higher parabolic edge along $x = a$ (SSCS)	Marked improvement	46
	(b) Lower parabolic edge along $x = 0$ (CSSS)	Marked improvement	49
	(c) One straight edge along $y = b$ (SSSC)	Marked improvement	52
2	(a) Two alternate edges including the higher and lower parabolic edges $x = 0$ and $x = a$ (CSCS)	Marked improvement	57
	(b) 2 straight edges along $y = 0$ and $y = b$ (SCSC)	Remarkable improvement	88
	(c) Any two edges except for the above option (CSSC, CCSS)	Marked improvement	63
3	3 edges including the two parabolic edges (CSCC, CCCS)	Marked improvement	45
	3 edges excluding the higher parabolic edge along $x = a$ (CCSC)	Remarkable improvement	96
4	All sides (CCCC)	Frequency attains the highest value	100

Table 6: Clamping options for +45/−45/+45/−45 conoidal shells with central cutouts having a'/a ratio 0.2.

Number of sides to be clamped	Clamped edges	Improvement of frequencies with respect to point supported shells	Marks indicating the efficiencies of number of restraints
0	Corner point supported	—	0
0	Simply supported no edges clamped (SSSS)	Marked improvement	52
1	(a) Higher parabolic edge along $x = a$ (SSCS)	Marked improvement	65
	(b) Lower parabolic edge along $x = 0$ (CSSS)	Marked improvement	64
	(c) One straight edge along $y = b$ (SSSC)	Marked improvement	66
2	(a) Two alternate edges including the higher and lower parabolic edges $x = 0$ and $x = a$ (CSCS)	Remarkable improvement	81
	(b) 2 straight edges along $y = 0$ and $y = b$ (SCSC)	Remarkable improvement	83
	(c) Any two edges except for the above option (CSSC, CCSS)	Remarkable improvement	77–79
3	3 edges including the two parabolic edges (CSCC, CCCS)	Remarkable improvement	86–89
	3 edges excluding the higher parabolic edge along $x = a$ (CCSC)	Frequency attains more than a fully clamped shell.	107
4	All sides (CCCC)	Remarkable improvement	100

5.2. Effect of Eccentricity of Cutout Position

5.2.1. Fundamental Frequency. The effect of eccentricity of cutout positions on fundamental frequencies is studied from the results obtained for different locations of a cutout with $a'/a = 0.2$. The non-dimensional coordinates of the cutout centre ($\overline{x} = x/a$, $\overline{y} = y/a$) were varied from 0.2 to 0.8 along each direction, so that the distance of a cutout margin from the shell boundary was not less than one tenth of the plan dimension of the shell. The margins of cutouts were stiffened with four stiffeners. The study was carried out for all the thirteen boundary conditions for both cross ply and angle ply shells. The fundamental frequency of a shell with an eccentric cutout is expressed as a percentage of fundamental frequency of a shell with a concentric cutout. This percentage is denoted by r. In Tables 7 and 8, such results are furnished.

It can be seen that eccentricity of the cutout along the length of the shell towards the parabolic edges makes it more flexible. It is also seen that towards the lower parabolic edge, r value is greater than that of the higher parabolic edge. This means that if a designer has to provide an eccentric cutout along the length, he should preferably place it towards the lower height boundary. The exception is there in some cases of cross ply shells. For cross ply shells with three edges simply

Table 7: Values of "r" for 0/90/0/90 conoidal shells.

Edge condition	$\overline{y}$	$\overline{x}$ 0.2	0.3	0.4	0.5	0.6	0.7	0.8
CCCC	0.2	82.951	90.621	99.503	101.707	93.088	85.111	79.437
	0.3	82.557	90.021	99.158	103.034	93.743	85.175	79.190
	0.4	81.946	89.117	97.773	101.280	92.554	84.271	78.405
	0.5	81.955	88.983	97.220	100.015	91.853	83.955	78.247
	0.6	81.946	89.115	97.771	101.280	92.555	84.271	78.405
	0.7	82.557	90.020	99.159	103.036	93.743	85.175	79.189
	0.8	82.887	90.511	99.407	101.694	93.070	85.088	79.424
CSCC	0.2	93.862	100.890	106.419	103.740	95.957	89.329	85.169
	0.3	96.374	104.672	110.505	108.656	101.815	94.918	89.726
	0.4	93.858	102.085	108.275	106.920	100.353	93.653	88.508
	0.5	90.589	97.867	102.329	100	93.876	88.419	84.453
	0.6	88.150	94.257	97.223	94.591	89.294	84.754	81.462
	0.7	87.105	92.080	94.299	92.0577	87.583	83.555	80.475
	0.8	87.065	91.375	93.317	91.458	87.383	83.527	80.519
CCSC	0.2	80.918	87.869	96.510	101.953	95.020	87.039	81.087
	0.3	80.426	87.123	95.768	102.726	95.727	87.269	81.107
	0.4	79.615	85.977	94.270	101.072	94.674	86.601	80.675
	0.5	79.448	85.705	93.791	100	93.987	86.365	80.627
	0.6	79.612	85.977	94.271	101.073	94.674	86.601	80.675
	0.7	80.426	87.122	95.770	102.726	95.727	87.268	81.106
	0.8	80.837	87.743	96.390	101.907	95.007	87.017	81.075
CCCS	0.2	87.175	91.751	93.546	91.679	87.294	83.462	80.475
	0.3	87.180	92.361	94.480	92.063	87.489	83.463	80.416
	0.4	88.309	94.562	97.427	94.587	89.193	84.660	81.409
	0.5	90.816	98.202	102.571	100	93.771	88.341	84.427
	0.6	94.105	102.438	108.564	106.999	100.349	93.673	88.565
	0.7	96.611	105.025	110.815	108.872	101.974	95.062	89.875
	0.8	93.762	101.038	106.545	103.958	96.168	89.383	85.123
CSSC	0.2	91.560	99.045	106.094	105.722	98.527	91.427	86.004
	0.3	91.466	99.489	107.457	108.698	103.151	96.316	90.410
	0.4	89.314	96.955	104.290	105.667	101.025	94.902	89.407
	0.5	88.004	95.094	100.516	100	95.159	90.036	85.737
	0.6	87.238	93.625	97.473	95.882	91.217	86.821	83.288
	0.7	87.033	92.615	95.568	94.032	89.939	85.975	82.704
	0.8	87.165	92.303	94.864	93.620	89.886	86.065	82.823
CCSS	0.2	87.339	92.674	95.098	93.607	89.769	85.968	82.749
	0.3	87.146	92.875	95.730	94.015	89.811	85.845	82.608
	0.4	87.407	93.903	97.657	95.859	91.084	86.689	83.196
	0.5	88.217	95.390	100.738	100	95.034	89.925	85.675
	0.6	89.541	97.258	104.563	105.762	101.012	94.895	89.435
	0.7	91.697	99.797	107.751	108.900	103.289	96.435	90.531
	0.8	91.033	98.862	106.134	105.856	98.729	91.447	85.903
CSCS	0.2	87.176	90.165	91.941	90.278	87.528	86.028	85.511
	0.3	90.236	93.667	95.133	93.168	90.295	88.544	87.299
	0.4	93.274	97.392	98.931	97.165	94.295	92.109	89.886
	0.5	95.713	99.837	101.259	100	97.767	96.416	93.011
	0.6	93.271	97.392	98.930	97.154	94.291	92.103	89.883
	0.7	90.232	93.666	95.133	96.907	90.294	88.544	87.296
	0.8	87.045	90.057	91.800	90.237	87.504	86.015	85.510

Table 7: Continued.

Edge condition	$\overline{y}$	$\overline{x}$ 0.2	0.3	0.4	0.5	0.6	0.7	0.8
SCSC	0.2	86.114	93.707	101.983	100.984	91.907	84.864	79.915
	0.3	85.570	92.996	101.670	102.014	92.324	84.978	79.910
	0.4	84.341	91.527	100.008	100.904	91.661	84.571	79.679
	0.5	83.782	90.945	99.224	100	91.321	84.472	79.663
	0.6	84.342	91.527	100.007	100.904	91.662	84.571	79.680
	0.7	85.570	92.996	101.673	102.014	92.325	84.979	79.911
	0.8	86.038	93.588	101.881	100.967	91.891	84.845	79.907
CSSS	0.2	90.957	94.019	96.237	95.319	93.007	91.535	90.574
	0.3	93.329	96.650	98.463	97.318	95.163	93.907	92.929
	0.4	94.987	98.154	99.743	99.094	97.663	96.789	95.576
	0.5	96.157	98.431	100.035	100	99.376	99.252	98.900
	0.6	94.984	98.155	99.743	99.092	97.661	96.784	95.572
	0.7	93.325	96.649	98.463	97.317	95.162	93.907	92.926
	0.8	90.826	93.898	96.032	95.227	92.974	91.510	90.575
SSSC	0.2	97.801	107.461	112.236	106.669	97.842	91.027	86.339
	0.3	100.320	109.209	113.744	109.522	101.475	94.421	89.126
	0.4	99.538	107.571	110.641	105.969	98.634	92.339	87.472
	0.5	97.804	105.127	105.975	100	93.276	88.232	84.425
	0.6	96.806	103.135	102.653	96.372	90.208	85.948	82.902
	0.7	96.657	101.965	101.055	95.197	89.518	85.604	82.855
	0.8	96.784	101.605	100.554	94.955	89.461	85.654	82.981
SSCS	0.2	93.160	96.470	95.571	91.662	88.790	87.812	87.727
	0.3	96.515	99.494	98.334	94.512	91.801	90.728	90.027
	0.4	99.292	102.150	101.314	97.900	95.242	93.801	92.363
	0.5	100.559	103.324	102.905	100	97.629	96.284	94.946
	0.6	99.290	102.155	101.314	97.896	95.240	93.802	92.362
	0.7	96.514	99.481	98.332	94.512	91.80	90.726	90.024
	0.8	93.059	96.355	95.442	91.626	88.753	87.798	87.733
SSSS	0.2	91.510	96.363	98.295	97.493	95.587	93.691	91.976
	0.3	95.252	98.790	99.925	98.895	97.114	95.560	94.407
	0.4	97.747	100.113	100.764	99.692	98.064	96.681	95.608
	0.5	98.751	100.497	101.006	100	98.510	97.233	96.154
	0.6	97.742	100.114	100.764	99.690	98.063	96.682	95.608
	0.7	95.251	98.786	99.922	98.897	97.113	95.560	94.405
	0.8	91.451	96.286	98.154	97.412	95.567	93.666	91.951
CS	0.2	137.892	128.050	114.295	104.647	100.791	101.361	109.077
	0.3	135.205	125.573	111.227	101.093	97.006	97.834	106.312
	0.4	132.315	124.337	110.519	100.187	95.990	97.045	105.585
	0.5	131.075	123.720	110.365	100	95.813	96.912	105.499
	0.6	132.292	124.356	110.550	100.211	96.017	97.088	105.603
	0.7	135.228	125.582	111.219	101.090	96.984	97.817	106.303
	0.8	135.480	125.754	112.435	102.528	98.801	99.577	107.915

$a/b = 1$, $a/h = 100$, $a'/b' = 1$, $a/h_h = 5$, $h_l/h_h = 0.25$, $E_{11}/E_{22} = 25$, $G_{23} = 0.2E_{22}$, $G_{13} = G_{12} = 0.5E_{22}$, and $\nu_{12} = \nu_{21} = 0.25$.

supported when cutout shifts towards the lower parabolic edge (including the lower parabolic edge) the shell becomes stiffer. Again for corner point supported shells, r values increase towards the parabolic edges and are maximum along lower parabolic edge. For cross ply shells, four out of thirteen boundary conditions yield the maximum value of r along $\overline{x} = 0.5$, four yield maximum values of r along $\overline{x} = 0.4$, and others show maximum values within $\overline{x} = 0.4$ to 0.5.

It is observed from Table 7 that if the eccentricity of a cutout is varied along the width, the shell becomes stiffer when the cutout shifts towards clamped edges. So, for functional purposes, if a shift of central cutout is required, eccentricity of a cutout along the width should preferably be towards the clamped straight edge. For shells having two straight edges of identical boundary condition, the maximum fundamental frequency occurs along $\overline{y} = 0.5$. For corner

Table 8: Values of "r" for +45/−45/+45/−45 conoidal shells.

Edge condition	$\overline{y}$	$\overline{x}$ 0.2	0.3	0.4	0.5	0.6	0.7	0.8
CCCC	0.2	72.823	78.236	82.758	83.828	81.568	76.803	71.923
	0.3	74.884	80.770	86.548	88.893	86.815	81.249	75.551
	0.4	76.701	83.522	91.226	95.703	93.788	87.111	80.040
	0.5	77.112	84.768	94.005	100	97.403	89.411	81.517
	0.6	76.805	83.652	91.325	95.680	93.763	87.160	80.108
	0.7	75.008	80.906	86.626	88.855	86.795	81.298	75.617
	0.8	72.647	77.908	82.266	83.759	81.579	76.633	71.755
CSCC	0.2	81.077	91.056	97.803	91.446	86.032	83.235	78.655
	0.3	83.525	93.130	102.170	99.590	94.922	89.192	82.211
	0.4	84.074	93.824	101.696	103.807	101.498	94.596	86.412
	0.5	83.003	90.427	97.733	100	99.474	96.299	87.547
	0.6	81.276	87.968	94.605	96.334	95.817	92.081	84.895
	0.7	79.646	86.287	92.866	94.104	92.136	86.701	80.220
	0.8	78.630	85.619	92.366	92.585	89.172	83.321	77.139
CCSC	0.2	70.077	77.727	85.937	83.800	79.229	74.361	69.326
	0.3	71.072	78.703	87.768	88.368	83.336	77.766	72.302
	0.4	71.984	80.017	89.895	95.290	89.759	82.905	76.264
	0.5	72.468	81.214	91.396	100	93.470	85.277	77.810
	0.6	71.937	79.893	89.673	95.311	89.871	83.044	76.355
	0.7	71.086	78.669	87.710	88.508	83.481	77.891	72.371
	0.8	70.006	77.569	85.788	83.973	79.340	74.231	69.123
CCCS	0.2	78.059	85.085	91.568	92.620	90.166	84.849	78.646
	0.3	78.792	85.576	91.983	93.758	92.489	87.571	81.169
	0.4	80.502	87.433	93.909	95.951	95.851	92.337	85.557
	0.5	82.841	90.481	97.657	100	99.876	96.861	88.986
	0.6	85.401	94.488	102.330	104.306	102.177	96.765	88.819
	0.7	85.313	94.803	103.136	100.952	96.520	91.365	84.617
	0.8	81.938	91.745	98.552	93.014	87.371	84.653	80.319
CSSC	0.2	80.251	90.347	102.001	98.147	92.559	90.103	85.813
	0.3	81.688	90.911	103.714	105.159	101.546	97.766	88.928
	0.4	81.340	89.735	99.850	103.865	102.503	98.783	91.054
	0.5	81.528	89.780	96.778	100	99.635	97.691	92.230
	0.6	81.914	89.289	95.251	97.877	98.401	97.867	92.317
	0.7	81.213	88.071	94.478	97.330	98.425	94.980	87.252
	0.8	80.276	87.186	94.253	97.479	97.826	90.750	83.637
CCSS	0.2	79.271	85.734	92.215	96.177	97.750	92.440	85.311
	0.3	80.024	86.471	92.663	96.147	97.781	95.350	88.242
	0.4	81.065	87.896	94.083	97.107	98.178	97.531	92.578
	0.5	82.087	90.360	97.023	100	100.117	98.606	94.251
	0.6	82.521	90.825	101.803	104.549	103.368	100.351	93.755
	0.7	82.941	91.821	103.719	105.727	102.486	99.509	91.399
	0.8	80.346	90.089	100.955	99.195	93.707	91.345	87.507
CSCS	0.2	78.163	86.022	92.995	92.450	88.854	85.808	80.401
	0.3	79.871	86.979	93.768	95.528	94.670	90.304	83.255
	0.4	81.380	88.475	95.483	97.758	98.510	95.335	87.720
	0.5	83.417	91.209	98.288	100	101.457	99.522	90.636
	0.6	83.285	90.593	97.462	99.337	99.875	96.908	89.038
	0.7	81.807	89.179	96.019	97.206	95.825	91.360	84.354
	0.8	79.311	87.551	94.710	93.330	88.907	85.864	80.620

Table 8: Continued.

Edge condition	$\overline{y}$	$\overline{x}$ 0.2	0.3	0.4	0.5	0.6	0.7	0.8
SCSC	0.2	85.127	94.329	95.136	88.093	85.184	82.426	78.466
	0.3	86.016	95.544	99.993	92.933	89.052	85.588	80.885
	0.4	86.853	97.202	105.501	97.941	92.882	88.930	83.293
	0.5	87.280	98.396	107.888	100	94.353	90.351	84.256
	0.6	86.654	96.782	104.675	97.456	92.684	88.887	83.209
	0.7	85.821	95.213	99.433	92.519	89.003	85.631	80.778
	0.8	84.798	93.899	94.867	87.932	85.323	82.385	78.165
CSSS	0.2	84.944	92.468	99.487	102.083	102.496	102.211	95.697
	0.3	87.001	94.415	100.612	101.921	103.359	105.519	99.083
	0.4	87.482	95.487	101.492	100.522	100.612	102.250	100.822
	0.5	87.931	97.254	102.629	100	99.420	100.620	99.680
	0.6	88.552	96.975	102.732	101.723	101.674	102.885	100.813
	0.7	88.608	96.436	102.875	103.969	105.120	106.825	99.475
	0.8	85.793	93.995	101.843	104.209	103.551	102.657	95.378
SSSC	0.2	90.301	101.510	103.781	96.224	91.653	89.271	87.137
	0.3	91.100	102.460	108.098	102.693	98.673	95.766	90.177
	0.4	90.295	101.404	106.028	102.757	98.698	95.253	90.038
	0.5	89.523	99.110	102.720	100	96.670	94.017	90.034
	0.6	88.793	96.857	100.664	98.472	96.351	94.739	91.563
	0.7	88.172	95.669	99.702	97.818	96.797	96.041	90.722
	0.8	87.395	94.930	98.931	96.571	95.997	95.427	88.365
SSCS	0.2	88.795	97.759	99.936	94.981	92.168	90.694	87.596
	0.3	90.150	98.974	101.928	98.665	97.216	96.201	89.404
	0.4	91.309	100.310	103.409	99.753	97.841	97.300	92.291
	0.5	92.288	101.662	104.357	100	97.487	96.678	93.643
	0.6	92.516	101.539	104.514	100.363	98.033	97.305	92.917
	0.7	91.859	100.918	103.929	99.899	98.067	97.444	90.291
	0.8	89.927	99.404	101.683	95.907	92.707	91.701	87.789
SSSS	0.2	88.805	93.985	97.537	99.443	99.34104	97.458	93.660
	0.3	90.116	95.853	98.238	99.300	99.55631	98.869	96.461
	0.4	89.799	95.332	98.006	97.770	96.847	96.012	94.848
	0.5	89.665	94.925	97.577	100	95.462	94.360	93.375
	0.6	90.247	95.512	98.509	98.722	97.792	96.672	95.013
	0.7	90.943	96.728	99.725	101.290	101.508	100.518	97.141
	0.8	88.912	94.653	99.280	101.663	101.056	99.261	95.529
CS	0.2	124.611	120.401	110.994	104.153	102.644	103.581	108.893
	0.3	120.487	117.591	108.489	101.849	100.596	101.659	107.324
	0.4	117.053	116.177	107.584	100.426	99.256	100.691	105.789
	0.5	115.794	115.786	107.429	100	98.788	100.425	105.330
	0.6	118.003	116.844	107.793	100.623	99.239	100.341	105.584
	0.7	122.490	118.779	109.260	102.384	100.470	100.978	106.534
	0.8	122.076	118.091	109.558	102.712	101.196	101.869	107.386

$a/b = 1$, $a/h = 100$, $a'/b' = 1$, $a/h_h = 5$, $h_l/h_h = 0.25$, $E_{11}/E_{22} = 25$, $G_{23} = 0.2E_{22}$, $G_{13} = G_{12} = 0.5E_{22}$, and $\nu_{12} = \nu_{21} = 0.25$.

point supported shells, the maximum fundamental frequency always occurs along the boundary of the shell. All these are true for cross ply shells only. For an angle ply shell, such unified trend is not observed, and the boundary conditions and the fundamental frequency behave in a complex manner as evident from Table 8. But for corner point supported angle-ply shells also, the maximum values of r are along the boundary.

Tables 9 and 10 provide the maximum values of r together with the position of the cutout. These tables also show the rectangular zones within which r is always greater than or equal to 95 and 90. It is to be noted that at some other points,

Table 9: Maximum values of r with corresponding coordinates of cutout centre and zones where $r \geq 90$ and $r \geq 95$ for 0/90/0/90 conoidal shells.

Boundary condition	Maximum values of r	Co-ordinate of cutout centre	Area in which the value of $r \geq 90$	Area in which the value of $r \geq 95$
CCCC	103.036	$\overline{x} = 0.5, \overline{y} = 0.7$	$\overline{x} = 0.6$, $0.2 \leq \overline{y} \leq 0.8$	$0.4 \leq \overline{x}\, 0.5$, $0.2 \leq \overline{y} \leq 0.8$
CSCC	110.505	$\overline{x} = 0.4, \overline{y} = 0.3$	$0.3 \leq \overline{x}\, 0.5$, $0.6 \leq \overline{y} \leq 0.8$	$0.3 \leq \overline{x}\, 0.6$, $0.2 \leq \overline{y} \leq 0.5$
CCSC	102.726	$\overline{x} = 0.5, \overline{y} = 0.3$ $\overline{x} = 0.5, \overline{y} = 0.7$	$\overline{x} = 0.4, 0.6$, $0.2 \leq \overline{y} \leq 0.8$	$\overline{x} = 0.5$, $0.2 \leq \overline{y} \leq 0.8$
CCCS	110.815	$\overline{x} = 0.4, \overline{y} = 0.7$	$0.3 \leq \overline{x}\, 0.5$, $0.2 \leq \overline{y} \leq 0.4$	$0.3 \leq \overline{x}\, 0.6$, $0.5 \leq \overline{y} \leq 0.8$
CSSC	108.698	$\overline{x} = 0.5, \overline{y} = 0.3$	$0.3 \leq \overline{x}\, 0.5$, $0.6 \leq \overline{y} \leq 0.8$	$0.3 \leq \overline{x}\, 0.6$, $0.2 \leq \overline{y} \leq 0.5$
CCSS	108.900	$\overline{x} = 0.5, \overline{y} = 0.7$	$0.3 \leq \overline{x}\, 0.5$, $0.2 \leq \overline{y} \leq 0.4$	$0.3 \leq \overline{x}\, 0.6$, $0.5 \leq \overline{y} \leq 0.8$
CSCS	101.259	$\overline{x} = 0.4, \overline{y} = 0.5$	$0.3 \leq \overline{x}\, 0.5$, $0.2 \leq \overline{y} \leq 0.3$ $0.7 \leq \overline{y} \leq 0.8$	$0.3 \leq \overline{x}\, 0.5$, $0.4 \leq \overline{y} \leq 0.6$
SCSC	102.014	$\overline{x} = 0.5, \overline{y} = 0.7$	$\overline{x} = 0.3, 0.5$, $0.2 \leq \overline{y} \leq 0.8$	$0.4 \leq \overline{x}\, 0.5$, $0.2 \leq \overline{y} \leq 0.8$
CSSS	100.035	$\overline{x} = 0.4, \overline{y} = 0.5$	$0.2 \leq \overline{x}\, 0.8$, $0.2 \leq \overline{y} \leq 0.8$	$0.3 \leq \overline{x}\, 0.6$, $0.3 \leq \overline{y} \leq 0.7$
SSSC	113.744	$\overline{x} = 0.4, \overline{y} = 0.3$	$0.6 \leq \overline{x}\, 0.7$, $0.2 \leq \overline{y} \leq 0.4$	$0.2 \leq \overline{x}\, 0.5$, $0.2 \leq \overline{y} \leq 0.8$
SSCS	103.324	$\overline{x} = 0.3, \overline{y} = 0.5$	$0.5 \leq \overline{x}\, 0.8$, $0.3 \leq \overline{y} \leq 0.7$	$0.2 \leq \overline{x}\, 0.4$, $0.3 \leq \overline{y} \leq 0.7$
SSSS	101.006	$\overline{x} = 0.4, \overline{y} = 0.5$	$\overline{x} = 0.8$, $0.2 \leq \overline{y} \leq 0.8$	$0.2 \leq \overline{x}\, 0.7$, $0.3 \leq \overline{y} \leq 0.7$
CS	137.892	$\overline{x} = 0.2, \overline{y} = 0.2$	nil	$0.2 \leq \overline{x}\, 0.8$, $0.2 \leq \overline{y} \leq 0.8$

$a/b = 1$, $a/h = 100$, $a'/b' = 1$, $a/h_h = 5$, $h_l/h_h = 0.25$, $E_{11}/E_{22} = 25$, $G_{23} = 0.2E_{22}$, $G_{13} = G_{12} = 0.5E_{22}$, and $\nu_{12} = \nu_{21} = 0.25$.

r values may have similar values, but only the zone rectangular in plan has been identified. This study identifies the specific zones within which the cutout centre may be moved so that the loss of frequency is less than 5% or 10%, respectively, with respect to a shell with a central cutout. This will help a practicing engineer to make a decision regarding the eccentricity of the cutout centre that can be allowed.

5.2.2. Mode Shapes. The mode shapes corresponding to the fundamental modes of vibration are plotted in Figures 6, 7, 8, and 9 for cross-ply and angle-ply shells of CCCC and CCSC shells for different eccentric positions of the cutout. As CCCC and CCSC shells are most efficient with respect to number of restraints, the mode shapes of these shells are shown as typical results. All the mode shapes are bending modes. It is found that for different position of cutout, mode shapes are somewhat similar, only the crest and trough positions change.

The present study considers the dynamic characteristics of stiffened composite conoidal shells with square cutout in terms of the natural frequency and mode shapes. The size of the cutouts and their positions with respect to the shell centre are varied for different edge constraints of cross-ply and angle-ply laminated composite conoids. The effects of these parametric variations on the fundamental frequencies and mode shapes are considered in details. However, the effect of the shape and orientation of the cutout on the dynamic characters of the conoid has not been considered in the present study. Future studies will evaluate these aspects.

6. Conclusions

The following conclusions are drawn from the present study.

(1) As this approach produces results in close agreement with those of the benchmark problems, the finite element code used here is suitable for analyzing free vibration problems of stiffened conoidal roof panels with cutouts. The present study reveals that cutouts with stiffened margins may always safely be provided on shell surfaces for functional requirements.

(2) The arrangement of boundary constraints along the four edges is far more important than their actual number; so far the free vibration is concerned. The relative-free vibration performances of shells for different combinations of edge conditions along the four sides are expected to be very useful in decision making for practicing engineers.

Table 10: Maximum values of r with corresponding coordinates of cutout centre and zones where $r \geq 90$ and $r \geq 95$ for +45/−45/+45/−45 conoidal shells.

Boundary condition	Maximum values of r	Co-ordinate of cutout centre	Area in which the value of $r \geq 90$	Area in which the value of $r \geq 95$
CCCC	100.000	$\overline{x} = 0.5, \overline{y} = 0.5$	$\overline{x} = 0.4, 0.6$ $0.4 \leq \overline{y} \leq 0.6$	$\overline{x} = 0.5,$ $0.4 \leq \overline{y} \leq 0.6$
CSCC	103.807	$\overline{x} = 0.5, \overline{y} = 0.4$	$\overline{x} = 0.3, 0.2 \leq \overline{y} \leq 0.5;$ $0.6 \leq \overline{x}\, 0.7, 0.3 \leq \overline{y} \leq 0.6$	$0.4 \leq \overline{x} \leq 0.5,$ $0.3 \leq \overline{y} \leq 0.5$
CCSC	100.000	$\overline{x} = 0.5, \overline{y} = 0.5$	$0.4 \leq \overline{x} \leq 0.6,$ $\overline{y} = 0.5$	$\overline{x} = 0.5$ $0.4 \leq \overline{y} \leq 0.6$
CCCS	104.306	$\overline{x} = 0.5, \overline{y} = 0.6$	$0.4 \leq \overline{x} \leq 0.6,$ $0.2 \leq \overline{y} \leq 0.4$	$0.4 \leq \overline{x} \leq 0.7,$ $0.5 \leq \overline{y} \leq 0.6$
CSSC	105.159	$\overline{x} = 0.5, \overline{y} = 0.3$	$0.4 \leq \overline{x} \leq 0.7,$ $0.7 \leq \overline{y} \leq 0.8;$ $\overline{x} = 0.8, 0.4 \leq \overline{y} \leq 0.6$	$0.4 \leq \overline{x} \leq 0.7,$ $0.3 \leq \overline{y} \leq 0.6$
CCSS	105.727	$\overline{x} = 0.5, \overline{y} = 0.7$	$\overline{x} = 0.5, 0.7$ $0.2 \leq \overline{y} \leq 0.4$ $\overline{x} = 0.3, 0.8$ $0.5 \leq \overline{y} \leq 0.7$	$0.5 \leq \overline{x} \leq 0.6,$ $0.2 \leq \overline{y} \leq 0.4$ $0.4 \leq \overline{x} \leq 0.7,$ $0.5 \leq \overline{y} \leq 0.7$
CSCS	101.457	$\overline{x} = 0.6, \overline{y} = 0.5$	$0.4 \leq \overline{x} \leq 0.7,$ $\overline{y} = 0.3$	$0.4 \leq \overline{x} \leq 0.7,$ $0.4 \leq \overline{y} \leq 0.7$
SCSC	107.888	$\overline{x} = 0.4, \overline{y} = 0.5$	$0.5 \leq \overline{x} \leq 0.6,$ $0.4 \leq \overline{y} \leq 0.6$	$0.3 \leq \overline{x} \leq 0.4,$ $0.3 \leq \overline{y} \leq 0.7$
CSSS	106.825	$\overline{x} = 0.7, \overline{y} = 0.7$	$\overline{x} = 0.3,$ $0.2 \leq \overline{y} \leq 0.8$	$0.4 \leq \overline{x} \leq 0.8,$ $0.2 \leq \overline{y} \leq 0.8$
SSSC	108.098	$\overline{x} = 0.4, \overline{y} = 0.3$	$0.7 \leq \overline{x} \leq 0.8,$ $0.3 \leq \overline{y} \leq 0.7$	$0.3 \leq \overline{x} \leq 0.6,$ $0.2 \leq \overline{y} \leq 0.7$
SSCS	104.514	$\overline{x} = 0.4, \overline{y} = 0.6$	$\overline{x} = 0.2, 0.8$ $0.3 \leq \overline{y} \leq 0.7$	$0.3 \leq \overline{x} \leq 0.7,$ $0.3 \leq \overline{y} \leq 0.7$
SSSS	101.663	$\overline{x} = 0.5, \overline{y} = 0.8$	$\overline{x} = 0.3, 0.8$ $0.2 \leq \overline{y} \leq 0.8$	$0.4 \leq \overline{x} \leq 0.7,$ $0.2 \leq \overline{y} \leq 0.8$
CS	124.611	$\overline{x} = 0.2, \overline{y} = 0.2$	nil	$0.2 \leq \overline{x}\, 0.8,$ $0.2 \leq \overline{y} \leq 0.8$

$a/b = 1$, $a/h = 100$, $a'/b' = 1$, $a/h_h = 5$, $h_l/h_h = 0.25$, $E_{11}/E_{22} = 25$, $G_{23} = 0.2E_{22}$, $G_{13} = G_{12} = 0.5E_{22}$, and $\nu_{12} = \nu_{21} = 0.25$.

(3) The information regarding the behaviour of stiffened conoids with eccentric cutouts for a wide spectrum of eccentricity and boundary conditions for cross ply and angle ply shells may also be used as design aids for structural engineers.

Notations

a, b: Length and width of shell in plan
a', b': Length and width of cutout in plan
b_{st}: Width of stiffener in general
b_{sx}, b_{sy}: Width of X- and Y-stiffeners, respectively
B_{sx}, B_{sy}: Strain-displacement matrix of stiffener elements
d_{st}: Depth of stiffener in general
d_{sx}, d_{sy}: Depth of X- and Y-stiffeners, respectively
$\{d_e\}$: Element displacement
e: Eccentricities of both x- and y-direction stiffeners with respect to shell midsurface
E_{11}, E_{22}: Elastic moduli
G_{12}, G_{13}, G_{23}: Shear moduli of a lamina with respect to 1, 2, and 3 axes of fibre
h: Shell thickness
h_h: Higher height of conoid
h_l: Lower height of conoid
M_x, M_y: Moment resultants
M_{xy}: Torsion resultant
np: Number of plies in a laminate
N_1–N_8: Shape functions
N_x, N_y: Inplane force resultants
N_{xy}: Inplane shear resultant
Q_x, Q_y: Transverse shear resultant
R_y, R_{xy}: Radii of curvature and cross curvature of shell, respectively
u, v, w: Translational degrees of freedom
x, y, z: Local coordinate axes
X, Y, Z: Global coordinate axes
z_k: Distance of bottom of the kth ply from midsurface of a laminate
α, β: Rotational degrees of freedom

ε_x, ε_y: Inplane strain component
ϕ: Angle of twist
γ_{xy}, γ_{xz}, γ_{yz}: Shearing strain components
ν_{12}, ν_{21}: Poisson's ratios
ξ, η, τ: Isoparametric coordinates
ρ: Density of material
σ_x, σ_y: Inplane stress components
τ_{xy}, τ_{xz}, τ_{yz}: Shearing stress components
ω: Natural frequency
$\overline{\omega}$: Nondimensional natural frequency $= \omega a^2 (\rho / E_{22} h^2)^{1/2}$.

References

[1] H. A. Hadid, *An analytical and experimental investigation into the bending theory of elastic conoidal shells [Ph.D. thesis]*, University of Southampton, 1964.

[2] C. Brebbia and H. Hadid, Analysis of plates and shells using rectangular curved elements, CE/5/71 Civil engineering department, University of Southampton, 1971.

[3] C. K. Choi, "A conoidal shell analysis by modified isoparametric element," *Computers and Structures*, vol. 18, no. 5, pp. 921–924, 1984.

[4] B. Ghosh and J. N. Bandyopadhyay, "Bending analysis of conoidal shells using curved quadratic isoparametric element," *Computers and Structures*, vol. 33, no. 3, pp. 717–728, 1989.

[5] B. Ghosh and J. N. Bandyopadhyay, "Approximate bending analysis of conoidal shells using the galerkin method," *Computers and Structures*, vol. 36, no. 5, pp. 801–805, 1990.

[6] A. Dey, J. N. Bandyopadhyay, and P. K. Sinha, "Finite element analysis of laminated composite conoidal shell structures," *Computers and Structures*, vol. 43, no. 3, pp. 469–476, 1992.

[7] A. K. Das and J. N. Bandyopadhyay, "Theoretical and experimental studies on conoidal shells," *Computers and Structures*, vol. 49, no. 3, pp. 531–536, 1993.

[8] D. Chakravorty, J. N. Bandyopadhyay, and P. K. Sinha, "Free vibration analysis of point-supported laminated composite doubly curved shells-A finite element approach," *Computers and Structures*, vol. 54, no. 2, pp. 191–198, 1995.

[9] D. Chakravorty, J. N. Bandyopadhyay, and P. K. Sinha, "Finite element free vibration analysis of point supported laminated composite cylindrical shells," *Journal of Sound and Vibration*, vol. 181, no. 1, pp. 43–52, 1995.

[10] D. Chakravorty, J. N. Bandyopadhyay, and P. K. Sinha, "Finite element free vibration analysis of doubly curved laminated composite shells," *Journal of Sound and Vibration*, vol. 191, no. 4, pp. 491–504, 1996.

[11] D. Chakravorty, P. K. Sinha, and J. N. Bandyopadhyay, "Applications of FEM on free and forced vibration of laminated shells," *Journal of Engineering Mechanics*, vol. 124, no. 1, pp. 1–8, 1998.

[12] A. N. Nayak and J. N. Bandyopadhyay, "On the free vibration of stiffened shallow shells," *Journal of Sound and Vibration*, vol. 255, no. 2, pp. 357–382, 2003.

[13] A. N. Nayak and J. N. Bandyopadhyay, "Free vibration analysis and design aids of stiffened conoidal shells," *Journal of Engineering Mechanics*, vol. 128, no. 4, pp. 419–427, 2002.

[14] A. N. Nayak and J. N. Bandyopadhyay, "Free vibration analysis of laminated stiffened shells," *Journal of Engineering Mechanics*, vol. 131, no. 1, pp. 100–105, 2005.

[15] A. N. Nayak and J. N. Bandyopadhyay, "Dynamic response analysis of stiffened conoidal shells," *Journal of Sound and Vibration*, vol. 291, no. 3–5, pp. 1288–1297, 2006.

[16] H. S. Das and D. Chakravorty, "Design aids and selection guidelines for composite conoidal shell roofs—a finite element application," *Journal of Reinforced Plastics and Composites*, vol. 26, no. 17, pp. 1793–1819, 2007.

[17] H. S. Das and D. Chakravorty, "Natural frequencies and mode shapes of composite conoids with complicated boundary conditions," *Journal of Reinforced Plastics and Composites*, vol. 27, no. 13, pp. 1397–1415, 2008.

[18] S. S. Hota and D. Chakravorty, "Free vibration of stiffened conoidal shell roofs with cutouts," *JVC/Journal of Vibration and Control*, vol. 13, no. 3, pp. 221–240, 2007.

[19] M. S. Qatu, E. Asadi, and W. Wang, "Review of recent literature on static analyses of composite shells: 2000–2010," *Open Journal of Composite Materials*, vol. 2, pp. 61–86, 2012.

[20] M. S. Qatu, R. W. Sullivan, and W. Wang, "Recent research advances on the dynamic analysis of composite shells: 2000–2009," *Composite Structures*, vol. 93, no. 1, pp. 14–31, 2010.

[21] V. V. Vasiliev, R. M. Jones, and L. L. Man, *Mechanics of Composite Structures*, Taylor and Francis, New York, NY, USA, 1993.

[22] M. S. Qatu, *Vibration of Laminated Shells and Plates*, Elsevier, London, UK, 2004.

[23] S. Sahoo and D. Chakravorty, "Finite element bending behaviour of composite hyperbolic paraboloidal shells with various edge conditions," *Journal of Strain Analysis for Engineering Design*, vol. 39, no. 5, pp. 499–513, 2004.